Electronic Supplementary Information (ESI)

Achieving High Singlet-Oxygen Generation by Applying Heavy-Atom Effect to Thermally Activated Delayed Fluorescent Materials

Ya-Fang Xiao,[a,d] Jia-Xiong Chen,[a,d] Wen-Cheng Chen,[b] Xiuli Zheng,[c,d] Chen Cao,[a,d] Jihua Tan,[a,d] Xiao Cui,[a,d] Zhanxiang Yuan,[b] Shaomin Ji,[b] Guihong Lu, *[e] Weimin Liu,[c,d] Pengfei Wang,[c,d] Shengliang Li*[a,d] and Chun-Sing Lee.*[a,d]*

[a] Center of Super-Diamond and Advanced Films (COSDAF) and Department of Chemistry, City University of Hong Kong, 999077, Hong Kong Special Administrative Region

[b] School of Chemical Engineering and Light Industry, Guangdong University of Technology, Guangzhou, 510006, P. R. China

[c] Technical Institute of Physics and Chemistry, Chinese Academy of Sciences, Beijing 100190, People's Republic of China

[d] Joint Laboratory of Nano-organic Functional Materials and Devices (TIPC and CityU), City University of Hong Kong, Kowloon, Hong Kong SAR, P. R. China

[e] State Key Laboratory of Biochemical Engineering, Institute of Process Engineering, Chinese Academy of Sciences, 1 North 2nd Street, Zhong Guan Cun, Beijing 100190, China.

Experimental Section

General information

All materials were purchased from commercial sources and used as received. DSPE-PEG2000, Hoechst 33342, 3-(4,5-dimethyl-2-thiazolyl)-2,5-diphenyl-2-*H*-tetrazolium bromide (MTT), Calcein acetoxymethyl ester (Calcein-AM) and Propidium Iodide (PI) were purchased from Sigma-Aldrich. Dulbecco's Modified Eagle Medium (DMEM), Phosphate-Buffered Saline (1×PBS, pH 7.4), Penicillin-Streptomycin (10, 000 U mL^{-1}), Fetal Bovine Serum (FBS), and Trypsin-EDTA (0.5%, no phenol red) were

purchased from Thermo Fisher Scientific. NMR spectra were recorded in $CDCl_3$ by a Bruker Advance-600 spectrometer, and mass spectra data were achieved *via* a GCT-TOF high-resolution mass spectrometer. Fluorescence spectra were measured using a Spectrofluorometer Fluormax-4 (HORIBA Jobin Yvon Inc.). Transient PL decay was measured using a spectrofluorometer of FLS980 (Edinburgh, UK). UV-Vis absorption spectra were recorded using an Ultra-Violet Visible Scanning Spectrophotometer Shimadzu 1700. Transmission electron microscopy (TEM) images were observed using an FEI / Philips Tecnai 12 BioTWIN. DLS analysis measurements were recorded using a Dynamic Light Scattering Particle Size Analyzer (Malvern Zetasizer Nano ZS). Fluorescence images of the cells were taken using a Laser Confocal Scanning Microscope (Leica SPE).

Synthesis

2-(4-(9H-carbazol-9-yl)phenyl)anthracene-9,10-dione (AQCz): 0.29 g of 2-bromoanthracene-9,10-dione (1 mmol), 0.34 g of (4-(9*H*-carbazol-9-yl)phenyl)boronic acid (1.2 mmol), 2.76 g of potassium carbonate (20 mmol), 23 mg of $Pd(PPh_3)_4$ (0.02 mmol) and 20 mL of 1,4-dioxane/H_2O (1:1) were added into a 100 ml three-necked flask under nitrogen atmosphere. Then, the mixture was stirred at 100 °C for 24 h. After cooled the mixture, added water and dichloromethane, and separated the organic layer and concentrated. The residue solid was purified by column chromatography to obtain the product (0.31g, 70%). ^{1}H NMR (600 MHz, $CDCl_3$) δ 8.64 (d, *J* = 1.9 Hz, 1H), 8.44 (d, *J* = 8.0 Hz, 1H), 8.36 (ddd, *J* = 6.2, 4.6, 2.2 Hz, 2H), 8.16 (d, *J* = 7.8 Hz, 2H), 8.12 (dd, *J* = 8.0, 1.9 Hz, 1H), 8.00 - 7.95 (m, 2H), 7.86 - 7.80 (m, 2H), 7.78 - 7.71 (m, 2H), 7.49 (d, *J* = 8.2 Hz, 2H), 7.47 - 7.41 (m, 2H), 7.34 - 7.28 (m, 2H). ^{13}C NMR (151 MHz, $CDCl_3$) δ 182.99, 182.65, 145.77, 140.64, 138.32, 137.86, 134.25, 134.12, 134.07, 133.69, 133.64, 132.42, 132.28, 128.84, 128.03, 127.41, 127.11, 127.05, 126.08, 125.38, 123.50, 120.28, 120.19, 109.77. GCT-TOF MS (mass m/z): 449.1409 $[M]^+$; calcd for $C_{32}H_{19}NO_2$ 449.1416. Anal. calcd for $C_{32}H_{19}NO_2$ C, 85.50; H, 4.26; N, 3.12; O, 7.12; found C, 85.32; H, 4.18; N, 3.01; O, 7.49.

2-(4-(3,6-dibromo-9H-carbazol-9-yl)phenyl)anthracene-9,10-dione (AQCzBr$_2$):

AQCz (0.23 g, 0.5 mmol) was added to 10 mL of *N*,*N*-dimethylformamide (DMF). Then slowly added 10 mL of DMF solution containing *N*-bromosuccinimide (0.22 g, 1.2 mmol), the reaction was stirred at room temperature for 12 h. After that, the mixture was poured into ice water bath and filtered, then washed with water, ethanol to get orange product (0.24g, 80%). ^{1}H NMR (600 MHz, $CDCl_3$) δ 8.63 (s, 1H), 8.45 (d, *J* = 8.0 Hz, 1H), 8.36 (s, 2H), 8.21 (s, 1H), 8.11 (d, *J* = 6.3 Hz, 1H), 7.98 (d, *J* = 8.3 Hz, 2H), 7.84 (s, 2H), 7.67 (d, *J* = 8.1 Hz, 2H), 7.54 (d, *J* = 10.0 Hz, 2H), 7.33 (d, *J* = 8.3 Hz, 3H). ^{13}C NMR measurement of $AQCzBr_2$ is not available due to its low solubility. GCT-TOF MS (mass m/z): 606.9594 $[M]^+$; calcd for $C_{32}H_{17}Br_2NO_2$ 606.9606. Anal. calcd for $C_{32}H_{17}Br_2NO_2$ C, 63.29; H, 2.82; Br, 26.31; N, 2.31; O, 5.27; found C, 63.11; H, 2.36; N, 2.24; O, 5.78; Br, 26.51.

Theoretical Calculations

Calculation on AQCz and $AQCzBr_2$ utilized density functional theory (DFT) as implemented in Orca 4.2.1 program package. Geometry optimization was performed with B3LYP functional using resolution of identity (RI) approximation without imposing any symmetry constraints in combination with the atom-pairwise dispersion corrections in the Becke-Johnson damping scheme (D3BJ). Basis set def2-TZVP and def2/J auxiliary basis were used for geometry optimizations on all atoms. Tight optimization and tight self-consistent field convergence with a fine Orca grid (Grid5, FinalGrid6) were employed on all geometry optimization calculations. Frequency calculation was performed on the equilibrium structure at the same level of theory to make sure local minimum of the geometry (without any imaginary frequency). Time-dependent DFT (used to calculate SOC parameters) using the Tamm-Dancoff approximation (TDA) was performed on the equilibrium structures with the identical set of geometry optimization.

Preparation of AQCz NPs and $AQCzBr_2$ NPs

250 μL of AQCz/THF (0.5 mg/mL) and 250 μL of DSPE-PEG2000/THF (5 mg/mL) were fully mixed and then added dropwise into 5 mL of DI water under 1200 rpm

magnetic stirring at 25°C for 1 h. Then THF was removed from the original AQCz NPs dispersions using a rotary evaporator. The AQCz NPs dispersions were stored at 4 °C for future use. $AQCzBr_2$ NPs was prepared using the same protocol of AQCz NPs.

Measurement and calculation of $^1O_2$ quantum yield (Φ_Δ)

Quantum yields of $^1O_2$ induced by TADF NPs were measured by using ABDA as a sensor under irradiation with a xenon lamp. The absorption of ABDA decreases proportionably with increased $^1O_2$ in the water phase. Methylene blue (MB) was used as a calibration standard (Φ_Δ = 52%). The decreased absorption of ABDA was monitored by an ultra-violet and visible spectrophotometer. All samples were irradiated with a xenon lamp of 50 mW/cm^2. The absorption maxima of MB and the TADF NPs were adjusted to ~ 0.1-0.3 OD. Φ_Δ of the TADF NPs were calculated using the following formula:

$$\Phi_\Delta(\text{sample}) = \frac{\Phi_\Delta(\text{MB}) \times K_{\text{sample}} \times A_{\text{MB}}}{K_{\text{MB}} \times A_{\text{sample}}}$$

where K_{sample} and K_{MB} are the decrease rate constants of the ABDA by the TADF NPs and MB at 399 nm, respectively. A_{MB} and A_{sample} represent the absorption integral of the MB and TADF NPs in the wavelength range 300-700 nm, respectively.

Detection of $^1O_2$ Generation *in vitro* and *in vivo*

For *in vitro* $^1O_2$ detection, the AQCz NPs ($AQCzBr_2$ NPs) were added into SOSG/DI water solution with the same area of integral absorption under white light irradiation (50 mW/cm^2) for different time intervals. The fluorescence intensity of DCFH was measured by the spectrofluorometer to investigate the ROS generation induced by one-photon laser. For *in vivo* $^1O_2$ detection, HeLa cells were seeded into 35 mm microscopy dishes with a glass bottom and treated with $AQCzBr_2$ NPs for 4 h. Then, all the cells were stained by the DCFH-DA/PBS solution for 30 min in 37 ℃ and then irradiated by white light under 50 mW/cm^2 for different time intervals. The fluorescence of DCFH-DA was observed by the CLSM and the fluorescence intensity of DCFH-DA in cells

was calculated by the CLSM software. The concentrations of AQCz NPs ($AQCzBr_2$ NPs) dispersions used in cell experiments represent the concentrations of AQCz ($AQCzBr_2$).

Cytotoxicity Assay

The cytotoxicity experiments were carried out using the MTT assay. HeLa cells or A549 cells (~ 5000 cells/well) were seeded on a 96-well plate in 100 μL of complete DMEM medium for 24 h incubation. The $AQCzBr_2$ NPs were diluted into different concentrations with 1×PBS. The cells were incubated with different concentrations of $AQCzBr_2$ NPs for 4 h and then irradiated under white light (50 mW/cm^2) for 5 min. After another 20 h, the cell viabilities were measured. To evaluate the dark cytotoxicity, the same concentrations of $AQCzBr_2$ NPs dispersions were added into HeLa cells or A549 cells in 96-well plate for 24 h in darkness, respectively, then the cell viabilities were measured. The values of IC50 were obtained by using the program of SPSS Data Editor.

Calcein AM/PI Assay

HeLa cells (~1×10^5/plate) were seeded in 35 mm plates and cultured for 12 h. Then, the cells were incubated with 10 μg/mL of $AQCzBr_2$ NPs for 4 h and then treated with or without white light (50 mW/cm^2, 5 min). After following 12 h, the cells were stained with Calcein AM/PI for 30 min and then washed twice with 1×PBS. The cells treated with the same volume of 1×PBS and only laser were taken as controls. Finally, all the group of cells were imaged by the Confocal Laser Scanning Microscope.

***In vivo* Antitumor Efficacy**

HeLa tumor-bearing mice (tumor volume=50-60 mm^3) were randomly divided into four groups (n = 5), including PBS, PBS + Laser (L), $AQCzBr_2$ NPs (NPs), and $AQCzBr_2$ NPs + Laser (NPs + L). 200 μL of $AQCzBr_2$ NPs (0.4 mg/mL) or 1 x PBS were *i.v* injected into mice and then two groups (L and NPs + L) of tumor were irradiated with Xenon lamp (150 mW/cm^2) for 5 min, and repeated the irradiation procedure 4 times

between a time interval of 2 minutes. The body weight and tumor volume of mice were measured every other day up to 18 days. At the end of the treatments, all the tumors were collected for the photograph.

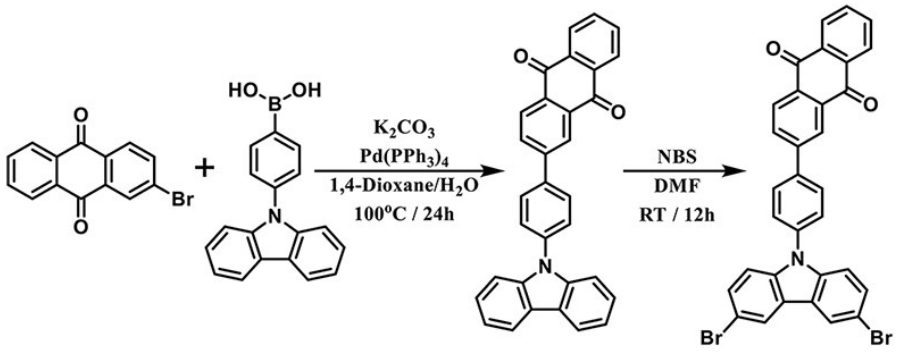

Scheme S1 Synthetic routes of AQCz and $AQCzBr_2$.

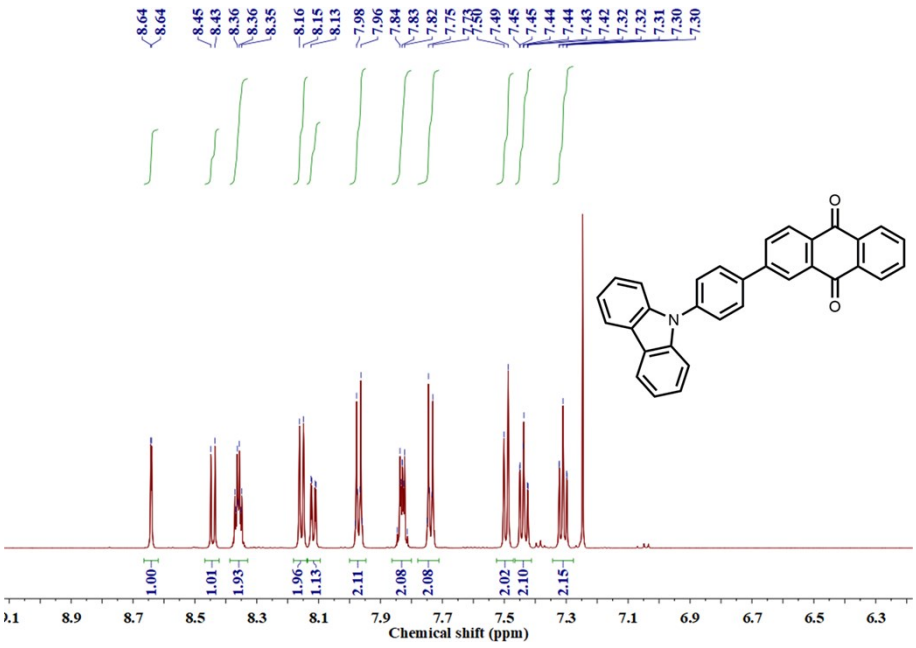

Fig. S1 ^1H NMR spectrum of AQCz in $CDCl_3$.

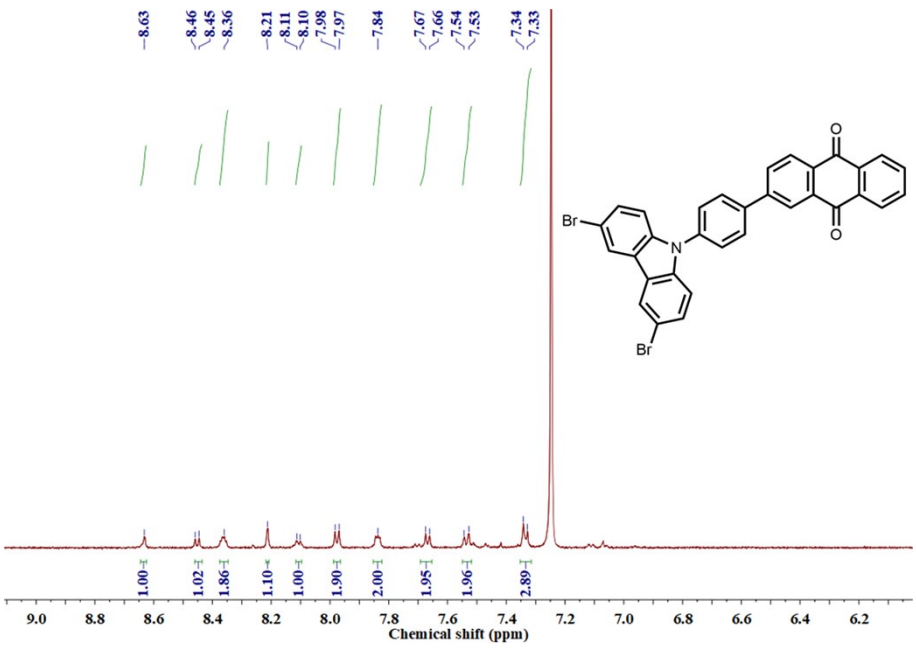

Fig. S2 ^{1}H NMR spectrum of $AQCzBr_2$ in $CDCl_3$.

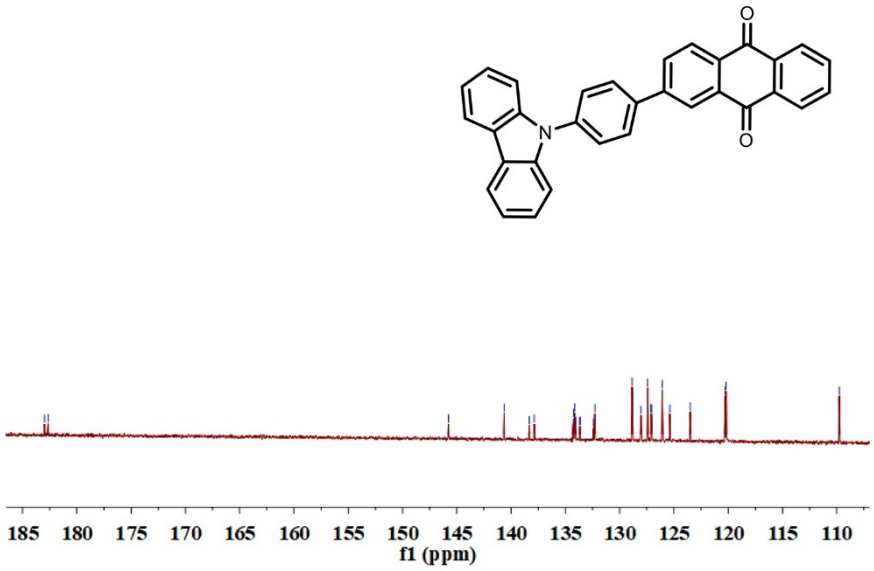

Fig. S3 ^{13}C-NMR spectrum of AQCz in $CDCl_3$.

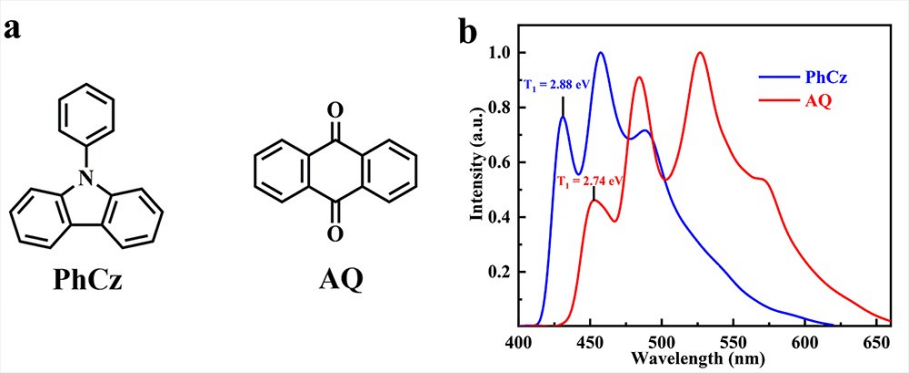

Fig. S4 (a) Chemical structures and (b) low-temperature phosphorescence spectra in THF at 77 K of PhCz and AQ.

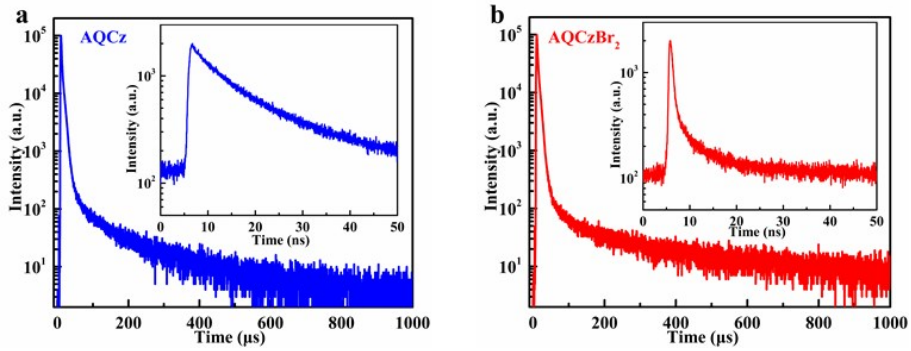

Fig. S5 Transient PL decay curves of 10 wt% (a) AQCz and (b) $AQCzBr_2$ doped PMMA thin films.

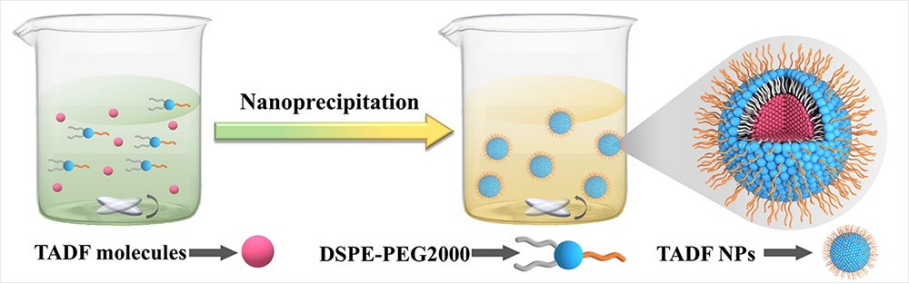

Fig. S6 Schematic illustration for nanoprecipitation of TADF NPs (AQCz NPs and $AQCzBr_2$ NPs).

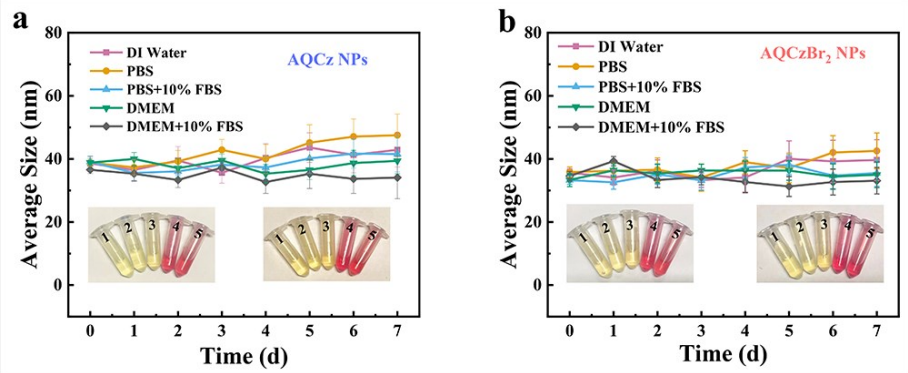

Fig. S7 Average sizes of (a) AQCz NPs and (b) $AQCzBr_2$ NPs in various media (1: DI water, 2: PBS, 3: PBS+10%FBS, 4: DMEM, 5: DMEM+10%FBS) during one week.

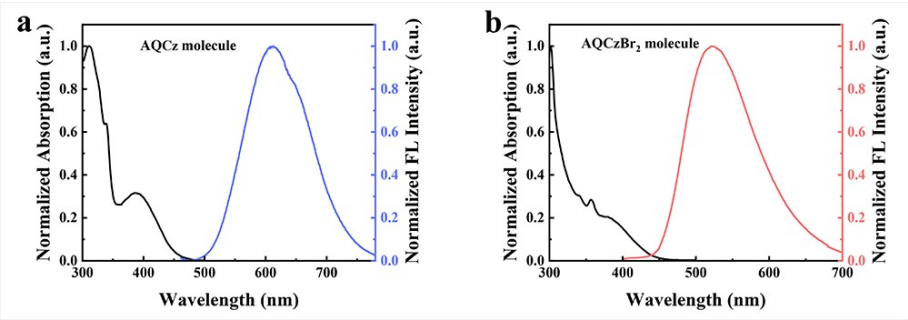

Fig. S8 Normalized absorption/fluorescence spectra of (a) AQCz and (b) $AQCzBr_2$ in THF.

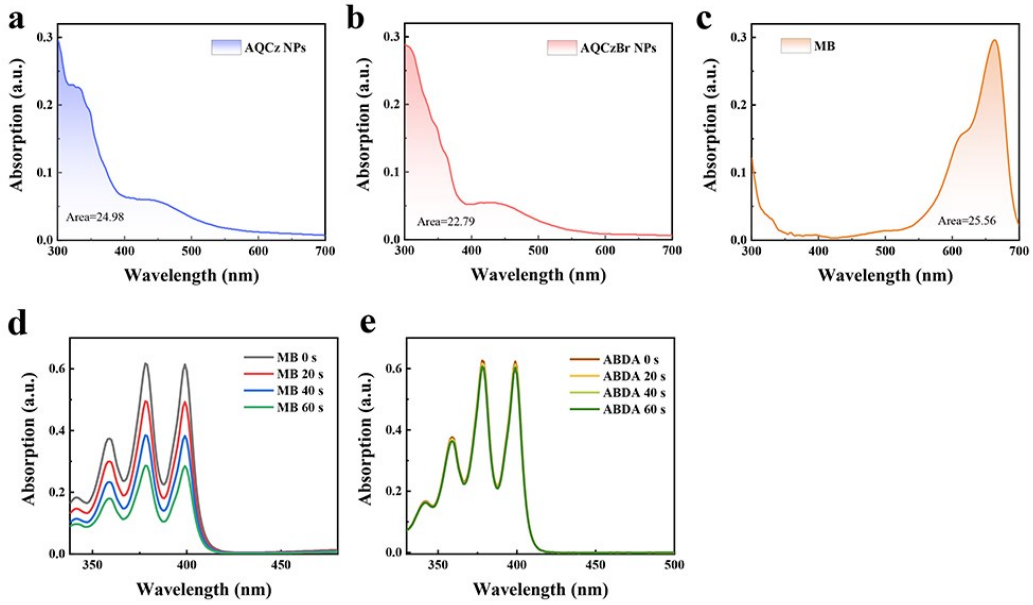

Fig. S9 Absorption spectra of (a) AQCz NPs, (b) $AQCzBr_2$ NPs and (c) MB, and the corresponding integral area. Time-dependent bleaching of ABDA caused by the $^1O_2$

generation of (d) MB and (e) PBS under white light irradiation.

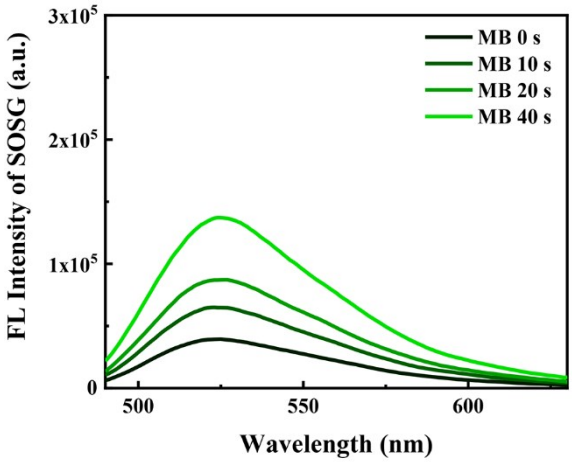

Fig. S10 Time-dependent enhancement of fluorescence of SOSG with the presence of MB.

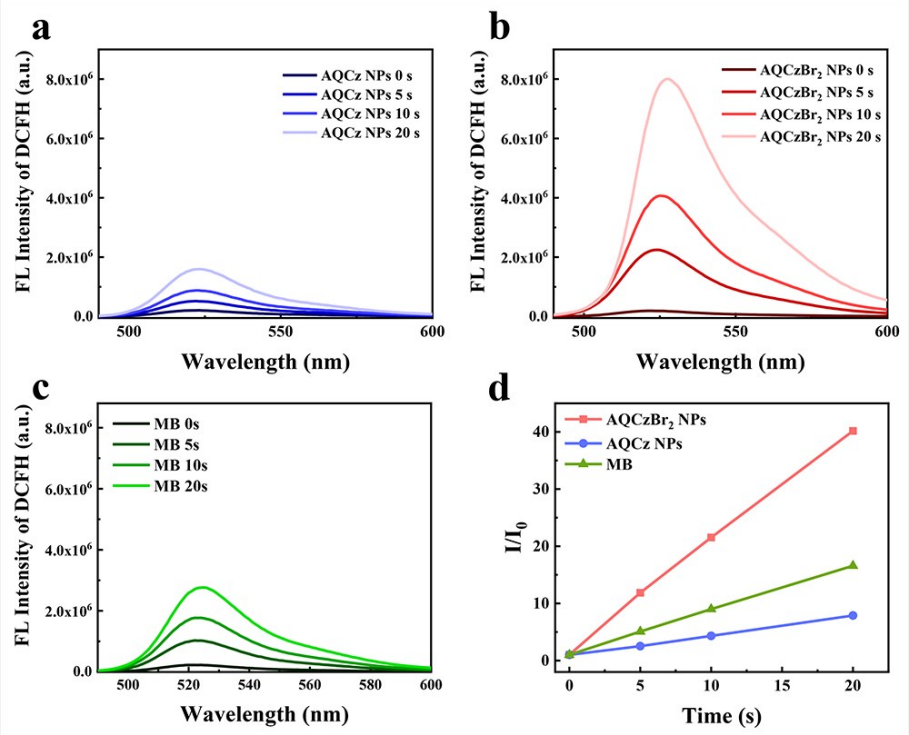

Fig. S11 Time-dependent enhancement of fluorescence of DCFH with the presence of (a) AQCz NPs, (b) $AQCzBr_2$ NPs and (c) MB under white light irradiation. (d) DCFH activated rates of AQCz NPs, $AQCzBr_2$ NPs and MB with the same area of integral absorption under white light irradiation. I_0 and I denote the fluorescence intensity of DCFH at 525 nm before and after light irradiation.

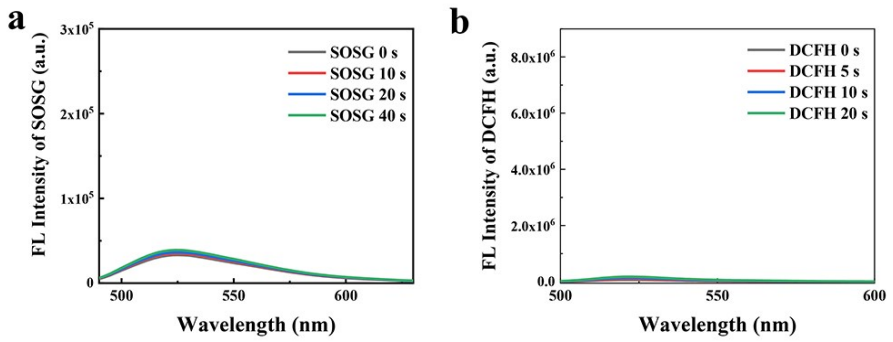

Fig. S12 Time-dependent enhancement of fluorescence of (a) SOSG and (b) DCFH caused by the $^1O_2$ generation of PBS under white light irradiation.

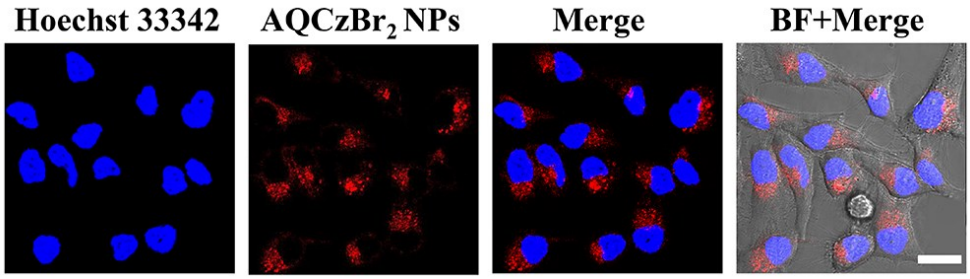

Fig. S13 Fluorescence confocal images of Hoechst 33342 (nuclear-specific dye) and $AQCzBr_2$ NPs (15 μg/mL) after 4-6 h incubation. BF: bright field. Scale bar = 20 μm

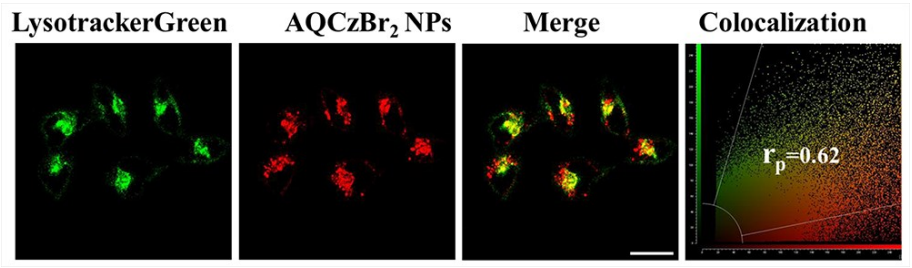

Fig. S14 Representative lysosome co-localization images of the $AQCzBr_2$ NPs in HeLa cells, where r_p indicates Pearson's co-localization coefficient. Scale bar = 20 μm.

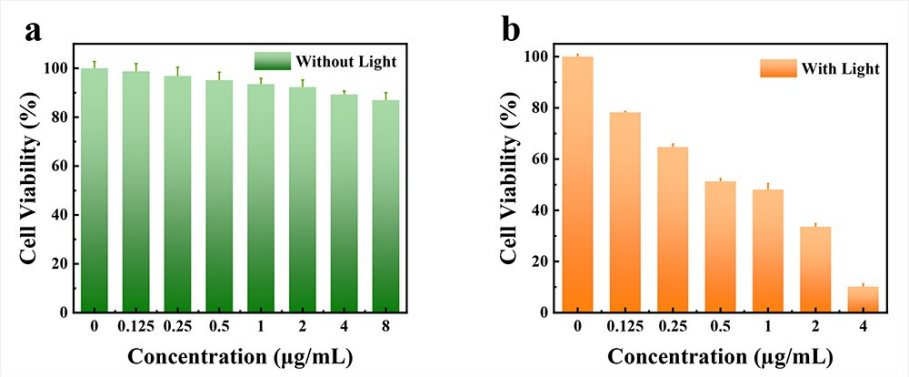

Fig. S15 (a) Dark-cytotoxicity and (b) photo-cytotoxicity of $AQCzBr_2$ NPs to A549 cells.

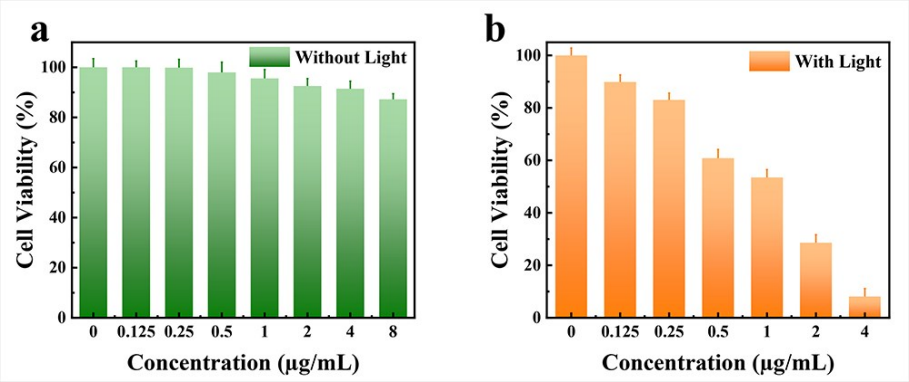

Fig. S16 (a) Dark-cytotoxicity and (b) photo-cytotoxicity of $AQCzBr_2$ NPs to NIH-3T3 cells.

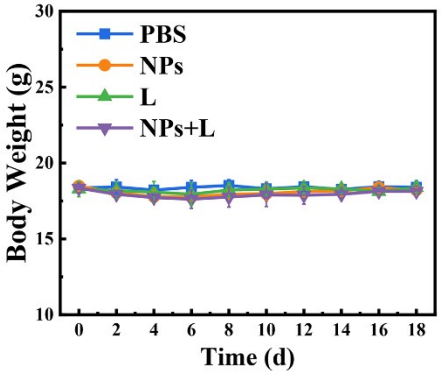

Fig. S17 Changes of body weight of mice from four groups during treatments.

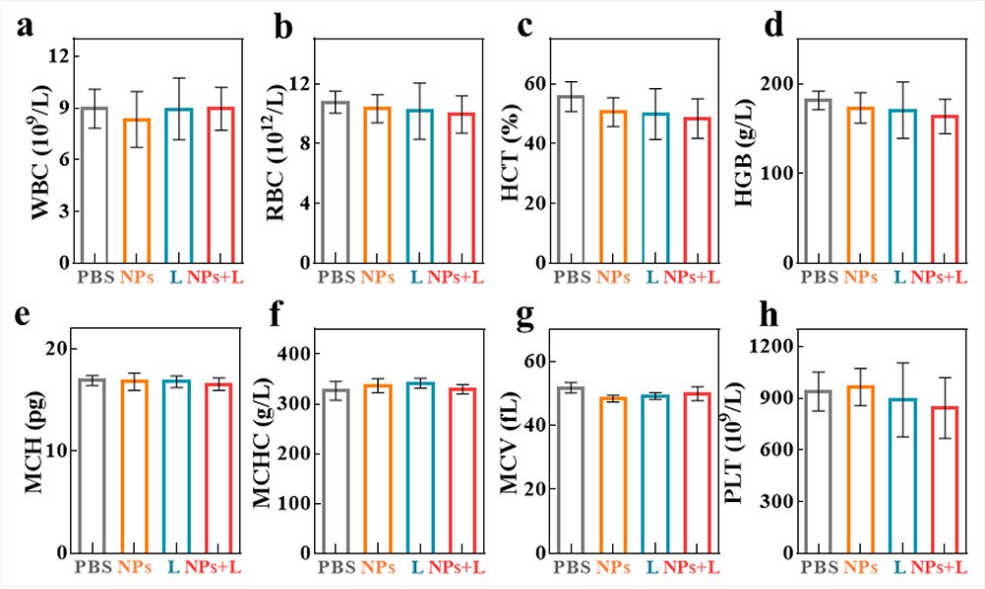

Fig. S18 Hematology analysis of mice after various treatments. (a) WBC: white blood cell count; (b) RBC: red blood cell count; (c) HCT: hematocrit; (d) HGB: hemoglobin; (e) MCH: mean corpuscular hemoglobin; (f) MCHC: mean corpuscular hemoglobin concentration; (g) MCV: mean corpuscular volume; (h) PLT: platelet count.

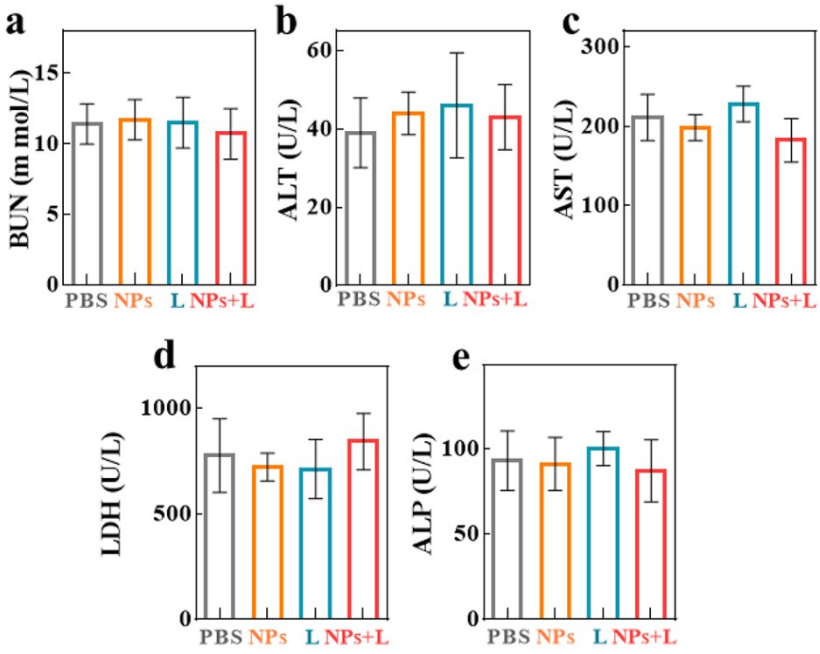

Fig. S19 Blood biochemistry analysis of mice after various treatments. (a) BUN: blood urea nitrogen; (b) ALT: total alanine aminotransferase; (c) AST: aspartate aminotransferase; (d) LDH: lactate dehydrogenase; (e) ALP: alkaline phosphatase.

Table S1. The values of ΔE_{ST} and $^1O_2$ quantum yield (QY) of various kinds of photosensitizers.

Material	ΔE_{ST} (eV)	$^1O_2$ QY (%)
Rose bengal	0.35 [1]	75 [2]
Chlorin e6	--	63 [3]
TPP (Porphyrin derivative)	--	67 [4]
Zinc(II) Phthalocyanine	1.1 [5]	67 [6]
BDP-4 (Bodipy derivative)	0.63 [7]	32 [7]
BDP-5 (Bodipy derivative)	0.44 [7]	68 [7]
TPPDC (TPE derivative)	0.35 [8]	32 [8]
PPDC (TPE derivative)	0.27 [8]	89 [8]
4CzIPN NPs (TADF material)	0.1 [9]	10.3 [9]
4CzTPN-Ph NPs (TADF material)	0.09 [9]	12.1 [9]
$AQCzBr_2$ NPs (TADF material)	0.11	91 (this work)

Table S2 Calculated values of S_1, T_1, ΔE_{ST} and $\xi(S_1\text{-}T_1)$ for AQCz and $AQCzBr_2$.

Compound	S_1 (eV)	T_1 (eV)	ΔE_{ST} (eV)	$\xi(S_1\text{-}T_1)$ (cm^{-1})
AQCz	2.34	2.23	0.11	0.10
$AQCzBr_2$	2.43	2.32	0.11	0.28

Reference:

1. J. M. Larkin, W. R. Donaldson, T. H. Foster and R. S. Knox, *Chem. Phys.* 1999, **244**, 319-330
2. F. Hu, S. Xu and B. Liu, *Adv. Mater.*, 2018, **30**, 1801350.
3. H. Mojzisova, S. Bonneau, P. Maillard, K. Berg and D. Brault, *Photoch. Photobio. Sci.*, 2009, **8**, 778.
4. M. Pineiro, A. L. Carvalho, M. M. Pereira A. M. d'A, R. Gonsalves, L. G. Arnaut and S. J. Formosinho, *Chem. Eur. J.* 1998, **4**, 2299-2307.
5. M. E. Alberto, B. C. Simone, G. Mazzone, E. Sicilia and N. Russo, *Phys. Chem.*

Chem. Phys. 2015, **17**. 23595-23601.

6. A. Ogunsipe, J.-Y. Chen and T. Nyokong, *New J. Chem.*, 2004, **28**, 822–827.
7. V. Nguyen, Y. Yim, S. Kim, B. Ryu, K. M. K. Swamy, G. Kim, N. Kwon, C. Kim, S. Park and J. Yoon, *Angew. Chem. Int. Ed.*, 2020, **59**, 8957–8962.
8. S. Xu, Y. Yuan, X. Cai, C.-J. Zhang, F. Hu, J. Liang, G. Zhang, D. Zhang and B. Liu, *Chem. Sci.*, 2015, **6**, 5824–5830.
9. J. Zhang, W. Chen, R. Chen, X.-K. Liu, Y. Xiong, S. V. Kershaw, A. L. Rogach, C. Adachi, X. Zhang and C.-S. Lee, *Chem. Commun.,* 2016, **52**, 11744–11747.